

The Reference Framework for System Simulations of the IEA SHC Task 44 / HPP Annex 38

Part B: Buildings and Space Heat Load

A technical report of subtask C

Report C1 Part B

Date: 06.09.2013, **Final - Revised**

By Ralf Dott¹, Michel Y. Haller², Jörn Ruschenburg³, Fabian Ochs⁴, Jacques Bony⁵

¹ Institut Energie am Bau - Fachhochschule Nordwestschweiz, IEBau - FHNW,
St. Jakobs-Strasse 84, CH-4132 Muttenz, Switzerland

Phone : +41 61 467 45 74

Fax : +41 61 467 45 43

E-mail : ralf.dott@fhnw.ch

² Institut für Solartechnik SPF, Hochschule für Technik HSR,
Oberseestr. 10, 8640 Rapperswil, Switzerland

³ Division Thermal Systems and Buildings, Fraunhofer-Institut für Solare
Energiesysteme ISE, Heidenhofstraße 2, 79110 Freiburg, Germany

⁴ Institut für Konstruktion und Materialwissenschaften, AB Energieeffizientes Bauen /
Bauphysik Universität Innsbruck, Technikerstr. 13, 6020 Innsbruck, Austria

⁵ Laboratoire d'énergétique solaire et de physique du bâtiment (LESBAT),
Avenue des Sports 20, 1401 Yverdon-les-Bains, Switzerland

IEA Solar Heating and Cooling Programme

The *International Energy Agency* (IEA) is an autonomous body within the framework of the Organization for Economic Co-operation and Development (OECD) based in Paris. Established in 1974 after the first “oil shock,” the IEA is committed to carrying out a comprehensive program of energy cooperation among its members and the Commission of the European Communities.

The IEA provides a legal framework, through IEA Implementing Agreements such as the *Solar Heating and Cooling Agreement*, for international collaboration in energy technology research and development (R&D) and deployment. This IEA experience has proved that such collaboration contributes significantly to faster technological progress, while reducing costs; to eliminating technological risks and duplication of efforts; and to creating numerous other benefits, such as swifter expansion of the knowledge base and easier harmonization of standards.

The *Solar Heating and Cooling Programme* was one of the first IEA Implementing Agreements to be established. Since 1977, its members have been collaborating to advance active solar and passive solar and their application in buildings and other areas, such as agriculture and industry. Current members are:

Australia	Finland	Singapore
Austria	France	South Africa
Belgium	Italy	Spain
Canada	Mexico	Sweden
Denmark	Netherlands	Switzerland
European Commission	Norway	United States
Germany	Portugal	

A total of 49 Tasks have been initiated, 35 of which have been completed. Each Task is managed by an Operating Agent from one of the participating countries. Overall control of the program rests with an Executive Committee comprised of one representative from each contracting party to the Implementing Agreement. In addition to the Task work, a number of special activities—Memorandum of Understanding with solar thermal trade organizations, statistics collection and analysis, conferences and workshops—have been undertaken.

Visit the Solar Heating and Cooling Programme website - www.iea-shc.org - to find more publications and to learn about the SHC Programme.

Current Tasks & Working Group:

Task 36	<i>Solar Resource Knowledge Management</i>
Task 39	<i>Polymeric Materials for Solar Thermal Applications</i>
Task 40	<i>Towards Net Zero Energy Solar Buildings</i>
Task 41	<i>Solar Energy and Architecture</i>
Task 42	<i>Compact Thermal Energy Storage</i>
Task 43	<i>Solar Rating and Certification Procedures</i>
Task 44	<i>Solar and Heat Pump Systems</i>
Task 45	<i>Large Systems: Solar Heating/Cooling Systems, Seasonal Storages, Heat Pumps</i>
Task 46	<i>Solar Resource Assessment and Forecasting</i>
Task 47	<i>Renovation of Non-Residential Buildings Towards Sustainable Standards</i>
Task 48	<i>Quality Assurance and Support Measures for Solar Cooling</i>
Task 49	<i>Solar Process Heat for Production and Advanced Applications</i>

Completed Tasks:

Task 1	<i>Investigation of the Performance of Solar Heating and Cooling Systems</i>
Task 2	<i>Coordination of Solar Heating and Cooling R&D</i>
Task 3	<i>Performance Testing of Solar Collectors</i>
Task 4	<i>Development of an Insolation Handbook and Instrument Package</i>
Task 5	<i>Use of Existing Meteorological Information for Solar Energy Application</i>
Task 6	<i>Performance of Solar Systems Using Evacuated Collectors</i>
Task 7	<i>Central Solar Heating Plants with Seasonal Storage</i>
Task 8	<i>Passive and Hybrid Solar Low Energy Buildings</i>
Task 9	<i>Solar Radiation and Pyranometry Studies</i>
Task 10	<i>Solar Materials R&D</i>
Task 11	<i>Passive and Hybrid Solar Commercial Buildings</i>
Task 12	<i>Building Energy Analysis and Design Tools for Solar Applications</i>
Task 13	<i>Advanced Solar Low Energy Buildings</i>
Task 14	<i>Advanced Active Solar Energy Systems</i>
Task 16	<i>Photovoltaics in Buildings</i>
Task 17	<i>Measuring and Modeling Spectral Radiation</i>
Task 18	<i>Advanced Glazing and Associated Materials for Solar and Building Applications</i>
Task 19	<i>Solar Air Systems</i>
Task 20	<i>Solar Energy in Building Renovation</i>
Task 21	<i>Daylight in Buildings</i>
Task 22	<i>Building Energy Analysis Tools</i>
Task 23	<i>Optimization of Solar Energy Use in Large Buildings</i>
Task 24	<i>Solar Procurement</i>
Task 25	<i>Solar Assisted Air Conditioning of Buildings</i>
Task 26	<i>Solar Combisystems</i>
Task 27	<i>Performance of Solar Facade Components</i>
Task 28	<i>Solar Sustainable Housing</i>
Task 29	<i>Solar Crop Drying</i>
Task 31	<i>Daylighting Buildings in the 21st Century</i>
Task 32	<i>Advanced Storage Concepts for Solar and Low Energy Buildings</i>
Task 33	<i>Solar Heat for Industrial Processes</i>
Task 34	<i>Testing and Validation of Building Energy Simulation Tools</i>
Task 35	<i>PV/Thermal Solar Systems</i>
Task 37	<i>Advanced Housing Renovation with Solar & Conservation</i>
Task 38	<i>Solar Thermal Cooling and Air Conditioning</i>

Completed Working Groups:

CSHPSS; ISOLDE; Materials in Solar Thermal Collectors; Evaluation of Task 13 Houses; Daylight Research



IEA Heat Pump Programme

This project was carried out within the Solar Heating and Cooling Programme and also within the *Heat Pump Programme*, HPP which is an Implementing agreement within the International Energy Agency, IEA. This project is called Task 44 in the *Solar Heating and Cooling Programme* and Annex 38 in the *Heat pump Programme*.

The Implementing Agreement for a Programme of Research, Development, Demonstration and Promotion of Heat Pumping Technologies (IA) forms the legal basis for the IEA Heat Pump Programme. Signatories of the IA are either governments or organizations designated by their respective governments to conduct programmes in the field of energy conservation.

Under the IA collaborative tasks or “Annexes” in the field of heat pumps are undertaken. These tasks are conducted on a cost-sharing and/or task-sharing basis by the participating countries. An Annex is in general coordinated by one country which acts as the Operating Agent (manager). Annexes have specific topics and work plans and operate for a specified period, usually several years. The objectives vary from information exchange to the development and implementation of technology. This report presents the results of one Annex. The Programme is governed by an Executive Committee, which monitors existing projects and identifies new areas where collaborative effort may be beneficial.

The IEA Heat Pump Centre

A central role within the IEA Heat Pump Programme is played by the IEA Heat Pump Centre (HPC). Consistent with the overall objective of the IA the HPC seeks to advance and disseminate knowledge about heat pumps, and promote their use wherever appropriate. Activities of the HPC include the production of a quarterly newsletter and the webpage, the organization of workshops, an inquiry service and a promotion programme. The HPC also publishes selected results from other Annexes, and this publication is one result of this activity.

For further information about the IEA Heat Pump Programme and for inquiries on heat pump issues in general contact the IEA Heat Pump Centre at the following address:

IEA Heat Pump Centre
Box 857
SE-501 15 BORÅS
Sweden
Phone: +46 10 16 55 12
Fax: +46 33 13 19 79

Visit the Heat Pump Programme website - <http://www.heatpumpcentre.org/> - to find more publications and to learn about the HPP Programme.

Legal Notice Neither the IEA Heat Pump Centre nor the SHC Programme nor any person acting on their behalf: (a) makes any warranty or representation, express or implied, with respect to the information contained in this report; or (b) assumes liabilities with respect to the use of, or damages, resulting from the use of this information. Reference herein to any specific commercial product, process, or service by trade name, trademark, manufacturer, or otherwise, does not necessarily constitute or imply its endorsement recommendation or favouring. The views and opinions of authors expressed herein do not necessarily state or reflect those of the IEA Programmes, or any of its employees. The information herein is presented in the authors' own words.

Contents

Executive Summary	1
1 Introduction	2
2 Reference Locations and Climate.....	2
3 Building geometries and thermal properties.....	3
3.1 Construction of building elements.....	6
3.2 Ground floor coupling.....	8
4 Loads	9
4.1 Ventilation	9
4.2 Shading.....	9
4.3 Internal load profiles.....	10
5 Heat emission system	12
6 Simulation Results.....	15
6.1 Weather data.....	15
6.2 Building energy balances and room temperatures.....	16
6.3 Monthly Heat loads	18
6.4 Flow and return temperatures	19
6.5 Tabular values of monthly building simulation results	21
7 Symbols	24
8 References.....	25
Appendix A: Temperature distribution and ambient design temperature.....	26
Appendix B: Long-wave radiation heat exchange with the sky.....	27
Appendix C: Heat load estimation	28
Appendix D: Ground Coupling Heat Losses (TRNSYS Type 985)	29
Appendix E: Return temperature control of heat distribution / heat pump	34
Appendix F: Changelog since first version of April 2012.....	35

Executive Summary

In Subtask C of the joint IEA Solar Heating and Cooling Programme Task 44 and Heat Pump Programme Annex 38 (T44A38), different concepts for solar and heat pump heating systems are evaluated based on annual system simulations. For these system simulations, common boundary conditions have to be defined in order to ensure that different performance obtained by the simulation of different system concepts are not a result of different boundary conditions used for the simulation. This report describes the definition of the reference space heat loads based on the definition of reference buildings and heat distribution systems. General boundary conditions such as climatic properties, domestic hot water load and properties of ground and boreholes for the simulation of ground heat exchangers are presented in Part A of this report (Haller et al. 2012).

Starting from the geometry of the single family house buildings that were defined in the IEA SHC Task 32, three reference buildings with different energetic performance have been defined for T44A38. These buildings are named SFH15, SFH45 and SFH100 according to their space heating energy demand which is approximately 15, 45 and 100 kWh/m²a (140 m² floor area) in the climate of Strasbourg.

Building geometry and construction data define the transmission of heat and solar radiation through the building envelope. Ventilation and shading characteristics as well as internal loads from occupants and electrical equipment are defined. A simplified approach is used for the calculation of the thermal ground coupling of the building.

The reference buildings have been implemented in the simulation platform TRNSYS and results from annual simulations are shown both as tabular values and as curves. For all implementations of this reference framework on other platforms it is important to check if the simulation results match the results shown in this report, which are also available in Excel-spreadsheets on the internal Task website.

The performance of both heat pumps and solar thermal systems depends significantly on the temperature levels of the heat demand. Therefore, for the comparison of the performance of a solar and heat pump system it is of utmost importance that the simulated flow and return temperatures of the heating system are comparable in the first place. This can be achieved by comparing curves of cumulated energy delivered vs. the temperature that marks the maximum of the flow or return temperature at the time of heat delivery. For the reference framework buildings presented in this report these curves are shown for the different climates of Strasbourg, Athens and Helsinki.

1 Introduction

This paper describes the three different reference buildings for the application in IEA SHC Task 44 / HPP Annex 38. All of the three buildings are sharing the same geometry, their main difference lies in the insulation layer thickness, thus the heat load. In addition, building SFH15 comes equipped with an air-to-air heat exchanger. The houses are named SFH (Single-Family House) 15, 45 and 100 according to their heat load for Strasbourg. The buildings are a modification of the IEA SHC Task 32 reference buildings (Heimrath & Haller 2007).

- SFH15 represents an actual building envelope with very high energetic quality. It fits the Swiss Minergie-P (Minergie 2010) and German Passivhaus (Feist 2005) requirements.
- SFH45 elements are constructed, such that they are oriented at actual legal requirements or represent a renovated building with good thermal quality of the building envelope.
- SFH100 represents a non renovated existing building.

The aim of this reference building description is to provide a simple basis for the comparison of system solutions in between the different projects of IEA SHC Task 44 / HPP Annex 38. Therefore the description considers partly very simple models that would not suit a thermal building simulation, but is sufficient for the use as heat load for the heat generator systems, considers all main heat flows and gives a basis for a more precise adaptation if it is necessary to show further effects of specific heat generator solutions.

Changes since the first "Final" version of this report are documented in Appendix F.

2 Reference Locations and Climate

Three locations for building simulations are chosen as reference within IEA SHC Task 44 / HPP Annex 38 "Solar and Heat Pumps". They were selected according to European directive of ecodesign requirements for energy-related products (Directive 2009/125/EC). These are namely Helsinki, Strasbourg and Athens. Davos and Montréal are proposed as additional, optional locations. Further information about the climate can be found in Haller et al. (2012).

The irradiation on inclined surfaces is calculated using the Perez model (Perez et al. 1990) with a standard ground reflectance of 0.2. The reflectance of the walls C and D (see Figure 3) is set 0.3. The sky temperature for the long-wave heat transfer is calculated using the Berdahl model (Martin & Berdahl) as described in Appendix B.

3 Building geometries and thermal properties

A general view of the building geometry and its orientation is shown in Figure 1. The orientation is given for the northern hemisphere¹. The common geometrical structure of the buildings is fixed by inside measures. The different buildings are then derived by applying the different wall thicknesses. The basic, independent, geometry is summarized in Table 1, the specific measures in Table 2. A view of the building's structure is given in Figure 2. Internal walls and floors are only depicted for the sake of completeness and play no active role in the simulation. The buildings are simulated as one common thermal zone, internal capacities caused by such building structures are simplified in the simulation as one 200 m² large inner wall, thus representing 400 m² of wall surface. Simulation is based on inside measurements, no additional thermal bridges are considered. The inner (air) volume of the buildings is 389.45 m³; the net floor area (first plus second floor) is 140 m² (Figure 2). The areas of the building envelope are summarized in Table 3.

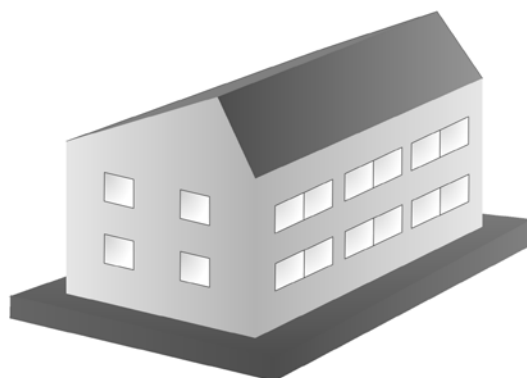


Figure 1: Simple view of the house (showing South and West facades).

Table 1: Building type independent geometry according to Figure 2.

part	a	b	f	g	h	m	n	r	α	β
measure	5.46 m	2.64 m	7 m	10 m	2.6 m	0.4 m	0.2 m	1.87 m	45°	20°

Table 2: Building type specific geometry according to Figure 2.

part	building	c	d	e	j	k	s
measure	SFH15	7.856 m	10.856 m	6.505 m	0.428 m	0.505 m	0.255 m
	SFH45	7.696 m	10.696 m	6.445 m	0.348 m	0.445 m	0.215 m
	SFH100	7.536 m	10.536 m	6.365 m	0.268 m	0.365 m	0.095 m

¹ For the southern hemisphere, the building shall be turned by 180°.

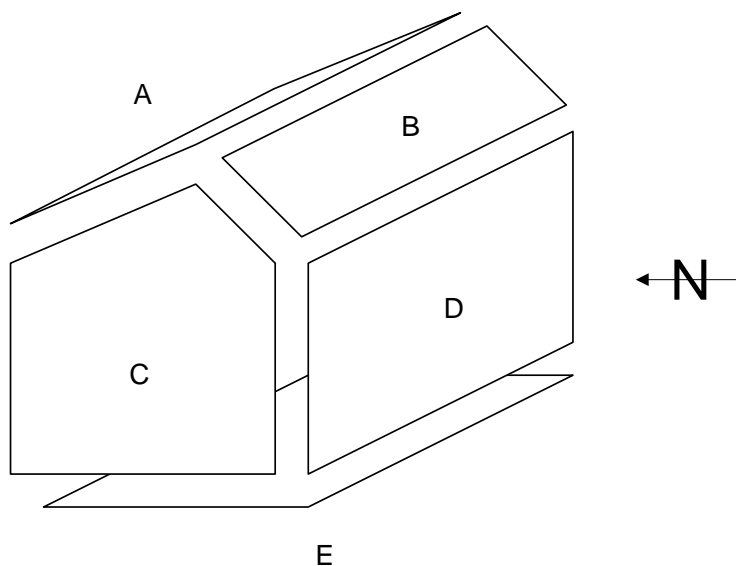


Figure 3: View of the envelope parts with naming convention for the areas.

Table 3: Inside and outside areas of the building envelope according to Figure 3.

	building	A =d*a	B =d*b	C =c*(e+r/2)	D =d*e	E =d*c
net (inside) area (m ²)	all	54.6	26.4	45.7	56.0	70.0
gross (outside) area (m ²)	SFH15	59.7	28.9	55.9	66.8	86.8
	SFH45	58.8	28.4	54.3	65.1	83.8
	SFH100	57.5	27.8	52.0	62.8	79.4

3.1 Construction of building elements

The construction of the building elements is described in detail in the following.

3.1.1 Opaque elements

The construction of the opaque elements (walls, floor, roof) is described in Table 4. U-value calculations are based on EN ISO 6946 (EN ISO 6946:2007), using a total heat transfer coefficient $\alpha_i=7.69 \text{ W/m}^2\text{K}$ to the inside and $\alpha_e=25.0 \text{ W/m}^2\text{K}$ to the outside (ambient). In simulations rather dynamic heat transfer coefficients (α_i & α_e), as e.g. shown in chapter 3.1.3, that also consider the heat flow direction instead of the static U-Values should be used.

Table 4: Construction of opaque building elements.

assembly	layer	layer thickness (m)			density (kg/m ³)	conduct. (W/mK)	capacity (kJ/kgK)	U-value construction (W/m ² K)		
		SFH15	SFH45	SFH100				SFH15	SFH45	SFH100
external wall	plaster inside	0.015	0.015	0.015	1200	0.600	1.00	0.182	0.286	0.667
	brick	0.210	0.210	0.210	1380	0.700	1.00			
	EPS	0.200	0.120	0.040	17	0.040	0.70			
	plaster outside	0.003	0.003	0.003	1800	0.700	1.00			
ground floor	wood	0.015	0.015	0.015	600	0.150	2.50	0.135	0.173	0.278
	plaster floor	0.080	0.080	0.080	2000	1.400	1.00			
	sound insul.	0.040	0.040	0.040	80	0.040	1.50			
	concrete	0.150	0.150	0.150	2000	1.330	1.08			
	XPS	0.220	0.160	0.080	38	0.037	1.45			
floor	wood	0.015	0.015	0.015	600	0.150	2.50	0.649	0.649	0.649
	plaster floor	0.080	0.080	0.080	2000	1.400	1.00			
	sound insul.	0.040	0.040	0.040	80	0.040	1.50			
	concrete	0.150	0.150	0.150	2000	1.330	1.08			
roof ceiling	gypsum board	0.025	0.025	0.025	900	0.211	1.00	0.162	0.197	0.575
	plywood	0.015	0.015	0.015	300	0.081	2.50			
	rockwool	0.200	0.160	0.040	60	0.036	1.03			
	plywood	0.015	0.015	0.015	300	0.081	2.50			
internal wall	clinker	0.200	0.200	0.200	650	0.230	0.92	0.885	0.885	0.885

If the simulation program used allows for their specification, the following values are used:

- The solar absorption is set 0.65 (both sides)
- the outer long-wave emission is 0.97 and the inner long-wave emission 0.96. The ceiling emission and the floor emission are set to 0.65.
- Sky view factors are 0.5 for all walls, 0.85 for the south facing roof, and 0.97 for the north facing roof (in agreement with the physical shape of the object and an open horizon).

3.1.2 Windows

The construction of the windows is given in Table 5 and their arrangement in Table 6, a simple view of the house with windows is provided in Figure 1. U-value calculations use the same total heat transfer coefficients of $\alpha_i=7.69 \text{ W/m}^2\text{K}$ to the inside and $\alpha_e=25.0 \text{ W/m}^2\text{K}$ to the outside (ambient) as for opaque elements. In simulations rather dynamic heat transfer coefficients (α_i & α_e) that also consider the heat flow direction instead of the static U-Values, as shown in chapter 3.1.3, should be used.

Table 5: Construction of windows.

building	construction (mm)	height (m)	width (m)	part frame	U_{glass} ($\text{W/m}^2\text{K}$)	U_{frame} ($\text{W/m}^2\text{K}$)	psi (W/mK)	tau _e	g-value	U_{tot} ($\text{W/m}^2\text{K}$)
SFH15	(4,16,4,16,4)	1	1		0.5	1.6	0.06	0.390	0.585	1.0
SFH45	(4,16,4)	1	1	15 %	1.1	1.8	0.06	0.415	0.622	1.5
SFH100	(4,16,4)	1	1		2.8	2.3	0.06	0.503	0.755	3.0

Table 6: Arrangement of the windows.

	window area (m^2)	glass area (m^2)	window quotient	opaque inside wall area (m^2)	total inside facade area (m^2)
North	3.0	2.6	5 %	53.0	56.0
East	4.0	3.4	9 %	41.7	45.7
South	12.0	10.2	21 %	44.0	56.0
West	4.0	3.4	9 %	41.7	45.7
Overall	23.0	19.6	11 %	180.5	203.5

3.1.3 Convective Heat Transfer Coefficients

The indoor convective heat transfer coefficients used for the reference simulation results could also be used for user implementation if not calculated automatically by the software. They are taken from Glück (2007) and calculated according to the following equations:

Horizontal surface, upward heat flux:
$$\alpha_c = 2.0 \frac{\text{W}}{\text{m}^2 \text{K}} \cdot \left| \mathcal{G}_{\text{surface}} - \mathcal{G}_{\text{air}} \right|^{0.31} \quad (1)$$

Horizontal surface, downward heat flux:
$$\alpha_c = 0.54 \frac{W}{m^2 K} \cdot \left| g_{surface} - g_{air} \right|^{0.31} \quad (2)$$

Vertical surface:
$$\alpha_c = 1.6 \frac{W}{m^2 K} \cdot \left| g_{surface} - g_{air} \right|^{0.3} \quad (3)$$

The outside surface convective heat transfer coefficients used for the reference simulation results are taken from EN ISO 6946 and calculated according to the following equation:

Outside surfaces:
$$\alpha_c = 4.0 \frac{W}{m^2 K} \cdot \frac{v_{wind}}{s} + 4 \frac{W}{m^2 K} \quad (4)$$

Where v_{wind} is the meteorological wind speed from the climate data.

3.2 Ground floor coupling

Ground floor coupling is calculated based on an approach described in ISO/DIS 13370. The detailed calculation procedure is described in the Appendix D. As a simplification, the following general inputs into this procedure are the same for all standard buildings of T44/A38. These are the length and width of the floor in contact with the ground ($l_{floor} = 10m$, $b_{floor} = 7m$), and the thickness of the sidewalls ($w = 0.4m$). The total heat transfer resistance of the ground slab is calculated based on the U-value of the floor as:

$$R_{tot} = 1/U_{floor} \quad (5)$$

Resulting values for U_{floor} , the average inside temperature of the room/floor $\bar{\theta}_i$, and its temperature variation over the year $\Delta\theta_i$, based on the climate of Strasbourg, are given in Table 7.

Table 7: Parameters for the calculation of ground coupling heat losses of the building.

building	all U_{floor} ^{a)} W/m ² K	Strasbourg		Athens		Helsinki		Davos		Montreal	
		$\bar{\theta}_i$ °C	$\Delta\theta_i$ K								
SFH015	0.141	23.8	3.8	23.3	3.3	24.2	4.2	24.2	4.2	24.0	4.0
SFH045	0.183	23.8	3.8	23.3	3.3	25.8	5.8	25.9	5.9	25.5	5.5
SFH100	0.278	20	0	20	0	20	0	20	0	20	0

a) U-value from active layer to ground in the case of SFH015 and SFH045 (i.e. not identical to U-value of floor construction in Table 4).

The values for $\bar{\theta}_i$ and $\Delta\theta_i$ reflect the particularity of floor heating (SFH15 and SFH45) and heating by radiators (SFH100). The procedure for obtaining these values is described in Appendix D.

4 Loads

4.1 Ventilation

A minimal, passive, constant air exchange rate of 0.4 h^{-1} , as fresh air demand of the building, is used. This constant air exchange takes place due to leakages at the houses SFH45 and SFH100. For the SFH15, the constant air exchange is due to mechanical ventilation which is modified by an air-to-air heat recovery. An adjustment of the fresh air temperature simulates this air-to-air heat exchanger with an effectiveness λ_{eff} of 0.6. This means that 0.6 of the difference between the temperatures \mathcal{G}_{room} of the outgoing air from the room and \mathcal{G}_{amb} of the outside (incoming) air is added to the incoming air temperature \mathcal{G}_{amb} .

$$\mathcal{G}_{out} = \mathcal{G}_{amb} + \lambda_{eff} \cdot (\mathcal{G}_{room} - \mathcal{G}_{amb}) \quad (6)$$

The air exchange due to tilted windows is also considered in the simulations and is added to the passive constant air exchange rate. A free driven night ventilation mode for passive cooling, realized by tilted windows, is activated for all buildings if all of the following conditions are met:

- Time between 9 p.m. and 8 a.m.
- average temperature of the last 24 hours above 12°C
- room temperature above 24°C
- ambient temperature at least 2K below the actual room temperature

The volume flow rate (m^3/s) for such a tilted window is calculated as

$$\dot{V}(\alpha) = C_d C_k(\alpha) \frac{W}{3} \sqrt{\frac{\Delta T}{T}} g H^3 \quad (7)$$

with the *discharge coefficient* $C_d = 0.0174\alpha - 0.0928HW^{-1} + 0.4116$ and the relative volume flow rate $C_k(\alpha) = 2.6 \cdot 10^{-7} \alpha^3 - 1.19 \cdot 10^{-4} \alpha^2 + 1.86 \cdot 10^{-2} \alpha$. Here H stands for the height and W for the width of the window, respectively. T is the average of the ambient and the room temperature (in Kelvin) and ΔT their difference, α is the opening angle of the window in degrees and g the acceleration of earth's gravity.

In case of meeting the stated conditions, six windows (1 m width, 1 m height), i.e. two on each facade except of the North, are tilted to an angle of 10° and the sum of the two ventilation rates is considered.

The direct window ventilation is only used as internal overheating protection. In this case the exchange rate is larger than 0.4 h^{-1} and the heat recovery ventilation uses a by-pass where the air from outside is directly inserted into the building without heat recovery.

4.2 Shading

All windows in the buildings are equipped with Venetian blinds. Those are activated, if all of the following conditions are met (off-values in parentheses):

- horizontal, global irradiation greater than 300 (200) W/m^2
- room temperature greater than 23.8 (22.8) $^\circ\text{C}$
- 24 hour moving average ambient temperature greater than 12°C

The shading is simulated by a constant factor of 0.25.

4.3 Internal load profiles

Two time dependent, internal gains are added in the building, on the one hand caused by inhabitants and on the other hand by electric equipment, described in the following sections.

4.3.1 Occupation profile

Gains caused by inhabitants are divided into convective (20 W) and radiative (40 W) gains per person. The latent heat of 40 W is included directly by the humidity with a mass flow of 0.059 kg/h. The occupation profile of the house is described by a factor changing every hour. The profile is identical for every day and is shown in Figure 4. The specific values can be found in Table 8. This corresponds to yearly values of 3.0 kWh/m²a convective and 6.0 kWh/m²a radiative gains.

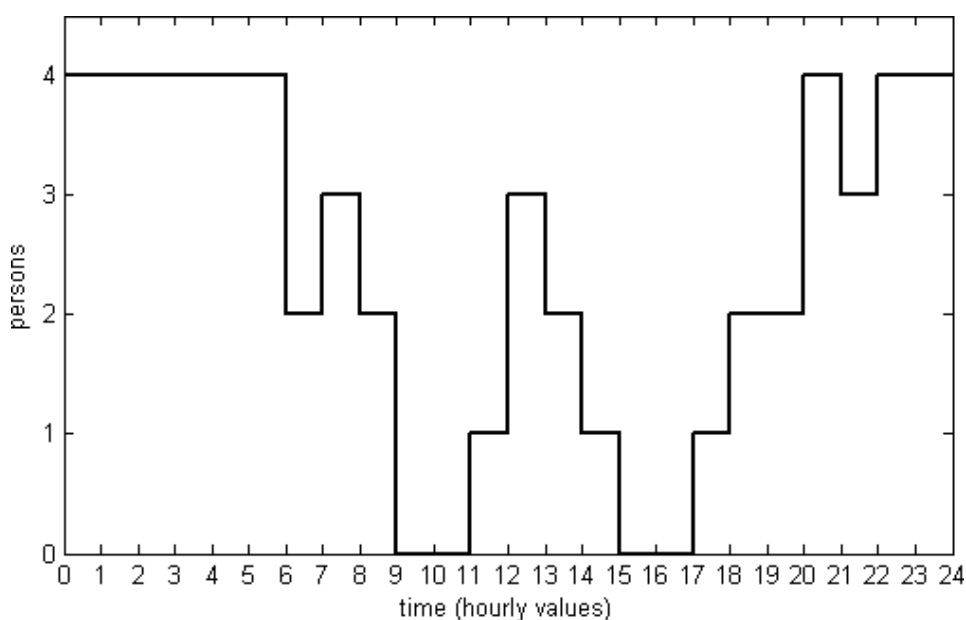


Figure 4: Occupation profile of a day, fraction of present persons.

4.3.2 Electrical gains profile

Thermal gains caused by the waste heat of electrical equipment are given by an external daily periodic profile, c.f. Figure 5. This electrical gains sum up to 13.4 kWh/m²a.

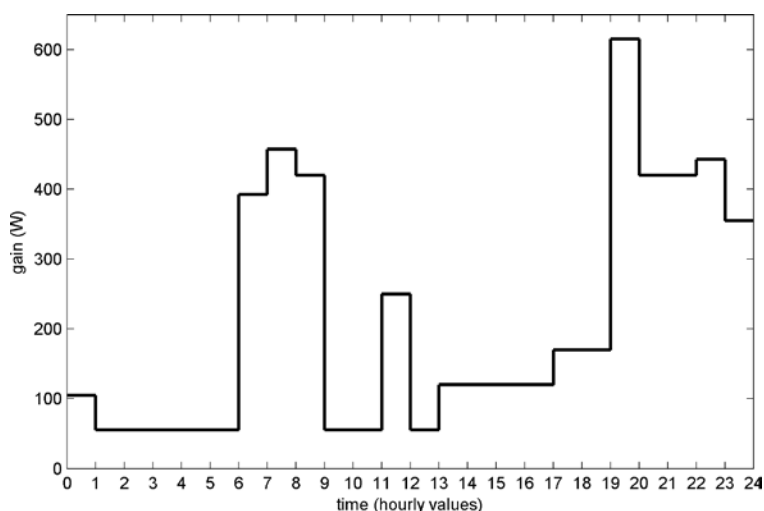


Figure 5: Electrical gain profile for one day.

Table 8: Electrical gains and occupation profile.

time (hour)	electricity gains (W)	occupation (persons)
0-1	105	4
1-2	55	4
2-3	55	4
3-4	55	4
4-5	55	4
5-6	55	4
6-7	392.5	2
7-8	457.5	3
8-9	420	2
9-10	55	0
10-11	55	0
11-12	250	1
12-13	55	3
13-14	120	2
14-15	120	1
15-16	120	0
16-17	120	0
17-18	170	1
18-19	170	2
19-20	615	2
20-21	420	4
21-22	420	3
22-23	442.5	4
23-0	355	4

5 Heat emission system

The controls of the heating system are set in a way, that the room temperature² is kept around $20 \pm 0.5^\circ\text{C}$ ($\mathcal{G}_{set} = 20^\circ\text{C}$) and never drops below 19.5°C during heating season. The design heating system parameters for the three houses are given in Table 9. The design outdoor temperatures \mathcal{G}_{ambD} have been derived as described in Appendix A and are -10.0°C for Strasbourg (ST), -1.0°C for Athens (AT) and -19.0°C for Helsinki (HE). \dot{Q}_{loc} is the standard heat load at design outdoor temperature for the given locations that has been derived as described in Appendix C. The design inlet temperature of the heat distribution system is given as $\mathcal{G}_{d,in}$ and the design outlet temperature as $\mathcal{G}_{d,out}$.

Table 9: Building dependent heating system parameters: design heat load, in- and outlet temperatures, and heating season limit.

building	$\dot{Q}_{loc,ST}$ (W)	$\dot{Q}_{loc,AT}$ (W)	$\dot{Q}_{loc,HE}$ (W)	$\mathcal{G}_{d,in,ST}$ (°C)	$\mathcal{G}_{d,out,ST}$ (°C)	$\mathcal{G}_{d,in,AT}$ (°C)	$\mathcal{G}_{d,out,AT}$ (°C)	$\mathcal{G}_{d,in,HE}$ (°C)	$\mathcal{G}_{d,out,HE}$ (°C)	\mathcal{G}_{HS} (°C)
SFH15	1'792	0	3'097	35	30	35	30	35	30	12
SFH45	4'072	1'310	6'315	35	30	35	30	40	35	14
SFH100	7'337	3'382	10'931	55	45	55	45	60	50	15

The supply temperature (inlet temperature) of the heating system (radiators or floor heating) is calculated as (Version 1):

$$\mathcal{G}_{in} = \mathcal{G}_{set} + \left(\frac{\dot{Q}_{Rd}}{\dot{Q}_{loc}} \right)^{\frac{1}{n_{Rd}}} \cdot \Delta \mathcal{G}_d + \frac{\dot{Q}_{Rd}}{2 \cdot \dot{m}_{max} \cdot c_{p(H_2O)}} \quad (8)$$

with the design heat load \dot{Q}_{loc} , $\Delta \mathcal{G}_d$ the difference of the mean of the radiator in- and outlet temperature and the room temperature setpoint \mathcal{G}_{set} (here $\mathcal{G}_{set} = 20^\circ\text{C}$), the assumed heating rate

$$\dot{Q}_{Rd} = \Theta(\mathcal{G}_{set} - \mathcal{G}_{amb24}) \cdot \dot{Q}_{loc} \cdot \frac{\mathcal{G}_{set} - \mathcal{G}_{amb24}}{\mathcal{G}_{set} - \mathcal{G}_{ambD}} \quad (9)$$

with the radiator exponent n_{Rd} , the specific heat of water $c_{p(H_2O)}$ and the maximal mass flow through the radiator

$$\dot{m}_{max} = \frac{\dot{Q}_{loc}}{c_{p(H_2O)} \cdot (\mathcal{G}_{d,in} - \mathcal{G}_{d,out})} \quad (10)$$

$\Theta(x)$ is the Heaviside-function, \mathcal{G}_{ambD} the *ambient design* temperature. For the calculation of the heating rate in equation (9) the ambient temperature \mathcal{G}_{amb24} is a 24 hours average value of the ambient temperature.

² For TRNSYS, the „convective“ room temperature is taken, not the „operative“ and not the „star node temperature“.

Alternatively to equation (8), the supply temperature of the heating system can be calculated as (Version 2):

$$\mathcal{G}_{in} = \mathcal{G}_{set} + \frac{\mathcal{G}_{d,in} - \mathcal{G}_{d,out}}{2} \cdot \frac{\mathcal{G}_{set} - \mathcal{G}_{amb24}}{\mathcal{G}_{set} - \mathcal{G}_{ambD}} + \left(\frac{\mathcal{G}_{d,in} + \mathcal{G}_{d,out}}{2} - \mathcal{G}_{set} \right) \cdot \left(\frac{\mathcal{G}_{set} - \mathcal{G}_{amb24}}{\mathcal{G}_{set} - \mathcal{G}_{ambD}} \right)^{\frac{1}{n_{Rd}}} \quad (11)$$

The mass flow through the heat distribution system is regulated by the simulation of a thermostatic valve with a PI and a P controller output signal that is multiplied with the maximum mass flow \dot{m}_{max} in order to obtain the actual mass flow that varies with time in each simulation. In the region of $\mathcal{G}_{set} \pm 1.5K$ the PI controller uses a proportional gain of $0.8 K^{-1}$, and an integral gain of $0.05 (Kh)^{-1}$. Outside of this band a P controller with a proportional gain of $0.5 K^{-1}$ is used (Heimrath & Haller 2007). This control setting is proposed for the reference building heat load³. Outside of the heating season, the space heat distribution pump is switched off. The criteria for the heating season are 24 hour averaged outdoor temperatures below the heating season limit \mathcal{G}_{HS} (Table 9). The On/Off control of the heat pump may need a return temperature setpoint for which the calculation is shown in Appendix E.

The space heat distribution pump has to be a pump that is able to overcome a pressure difference of 0.3 bar^4 at the nominal flow rate of the heating system \dot{m}_{max} . The electric energy needed for this pump has to be simulated according to this rule. Reduced mass flow rates do not automatically lead to el. power reduction of the reference systems because they are assumed to be a result of increased pressure drop due to thermostatic valves. If a detailed calculation of pressure drops and electricity demand for pumping is used that differs from these rules the details and the differences in results shall be laid open.

5.1.1 Radiator for SFH100

To simulate the heat transfer to the SFH100 building for space heating a radiator is used. The radiative fraction of emitted power is 0^5 , a radiator exponent $n_{Rd} = 1.3$ and a thermal capacitance of $1'150 \text{ kJ/K}$ are used. The nominal radiator power is 1.3 times the design heat load for the desired location.

³ Different control strategies for the mass flow in the heat distribution system can be chosen, assuming no thermostatic valves in some or in all loops. However, this may have an influence on the flow and return temperatures, on the heat load, on the seasonal performance factor, and on the electricity demand of the system. Whenever a different mass flow control is chosen, the strategy has to be explained in detail, and the resulting frequencies of room temperatures, flow temperatures and return temperatures are to be compared with the reference. Care has to be taken with the interpretation of the results since avoiding thermostatic valves may increase the seasonal performance factor while at the same time increasing the amount of heat emitted and thus the the total electricity demand of the system. Consequently, a better seasonal performance factor may be achieved for a solution that has more electricity demand and is therefore less efficient.

⁴ 0.25 bar for the heat distribution system and 0.05 bar for pressure drops within the hydraulics of the central heating units and their connections

⁵ The value 0 was introduced because of the limitations in some simulation programs and then kept by accident. 0.35 would be more realistic, but the results of the simulations may be different and therefore the value was not updated anymore during the course of the IEA Task.

5.1.2 Floor heating system for SFH45 and SFH 15

As floor heating system a 0.08 m thick active layer with pipes at 0.04 m depth in the floor is used. The pipes have an outer diameter of 0.016 m and a wall thickness of 0.002 m. Pipes are lying in the floor with a mutual distance of 0.1 m, thus giving a total pipe length of 700 m for one (70 m²) floor. The conductivity of the pipes is assumed to be 0.35 W/mK and the conductivity of the layer material 1.4 W/mK. The used fluid is water.

For SFH45 and SFH15, floor heating can be simulated within a building model that has the capability for it. However, in the reference simulations performed with TRNSYS, for the sake of simplicity, a floor heating system was approximated in simulations by using an ordinary room radiator model. In this case, the radiator exponent n_{Rd} was set to 1.1 and the thermal capacitance was raised to 40'000 kJ/K to simulate the inertia of a floor. The nominal radiator power is also 1.3 times the design heat load. In this case, because the thermal capacitance of the floor is already included in the radiator, no additional thermal capacitance for the floor has been included in the building model.

The inlet temperature is calculated in the same way as before in equation 8 or equation 11, the nominal mass flow rate according to equation 10.

6 Simulation Results

6.1 Weather data

The weather data for Strasbourg is analyzed in more detail in this section. Table 10 shows monthly values for the irradiation (diffuse and direct) for a south facing wall and for a surface with an inclination of 45° facing south, as well as monthly averaged temperatures for the temperature difference between the effective sky temperature and the ambient and the temperature of the undisturbed ground in 2 meter depth. Graphical representations of monthly irradiances are shown in Figure 6.

Table 10: Selected monthly values for irradiation on building surfaces, sky temperature difference and ground temperature for the climate of Strasbourg.

	South		45south		dTsky K	Tgrd2 °C
	direct kWh/m2	diffuse kWh/m2	direct kWh/m2	diffuse kWh/m2		
Jan	23.1	17.6	20.6	21.9	-6.71	7.00
Feb	29.7	29.2	35.5	30.6	-7.16	6.17
Mar	48.1	38.5	48.5	59.5	-8.79	6.59
Apr	34.4	50.3	68.8	60.2	-8.14	8.19
May	31.6	51.7	71.7	76.0	-8.54	10.57
Jun	23.1	54.6	79.4	66.3	-7.48	13.07
Jul	25.5	58.0	83.9	68.9	-6.90	15.03
Aug	36.7	54.6	75.1	73.7	-7.06	15.92
Sep	44.8	43.6	56.4	64.0	-7.18	15.48
Oct	40.9	31.2	38.2	44.2	-6.86	13.84
Nov	25.1	20.8	24.4	23.6	-6.64	11.45
Dec	20.7	14.5	16.9	18.8	-6.88	8.95
Total	383.7	464.6	619.7	607.7	-7.36	11.05

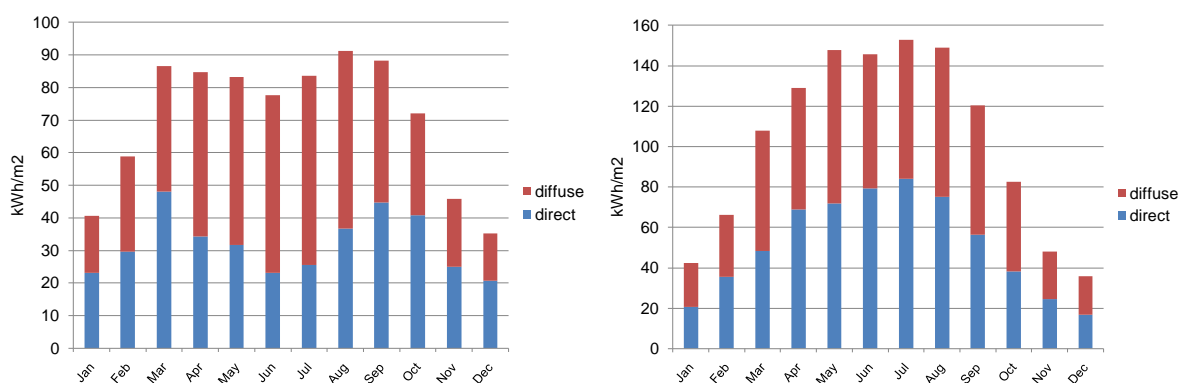


Figure 6: Direct solar and diffuse (also reflected) solar irradiation on a south facing wall (left) and for the 45° inclined surface facing to south (right) for the climate of Strasbourg.

6.2 Building energy balances and room temperatures

Version 2 (equation 11) has been used to calculate the supply temperature setpoint of the heat distribution system and all simulations have been performed with thermostatic valves by PI control of the mass flow rates. The energy balances for the SFH15, SFH45, and SFH100 in the climate of Strasbourg are shown in Figure 7. Additional energy balances for the SFH 45 are shown in Figure 8 for the climates of Athens and Helsinki. The heat load of the SFH 45 in the climate of Athens is extremely low, and it seems quite unlikely that this heat load at this location will be a candidate for a combined solar & heat pump system. Therefore, only values for the SFH 100 will be shown for the climate of Athens in subsequent sections. The transmission losses shown do not include ground heat exchange losses since these are shown separately. The distribution of hourly averaged room temperatures⁶ for the different building simulations in the different climates is shown in Figure 9 and Figure 10.

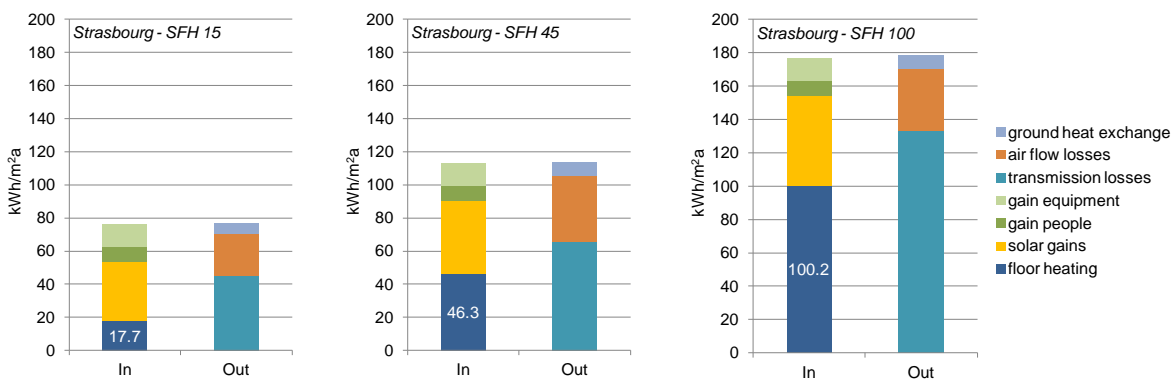


Figure 7: Resulting building energy balances for the three different houses at the climate of Strasbourg.

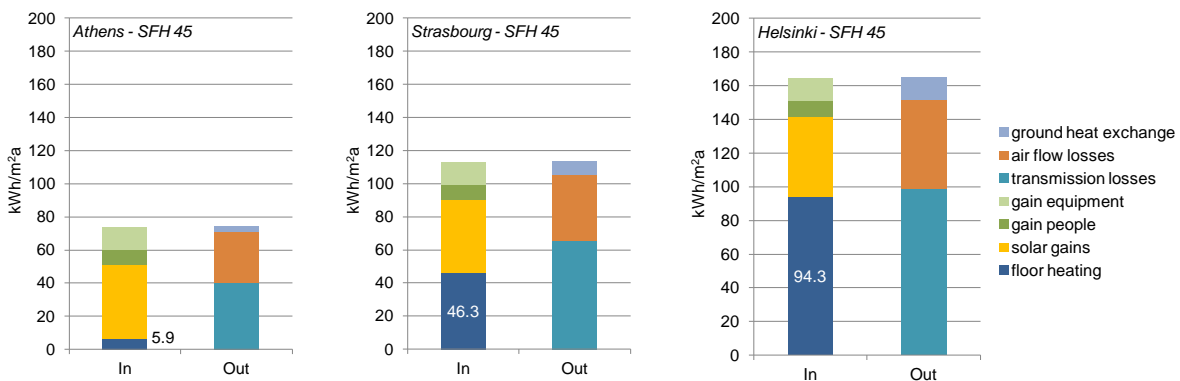


Figure 8: Resulting building energy balances of the SFH 45 at three different locations.

⁶ For TRNSYS, the „convective“ room temperature is taken, not the „operative“ and not the „star node temperature“.

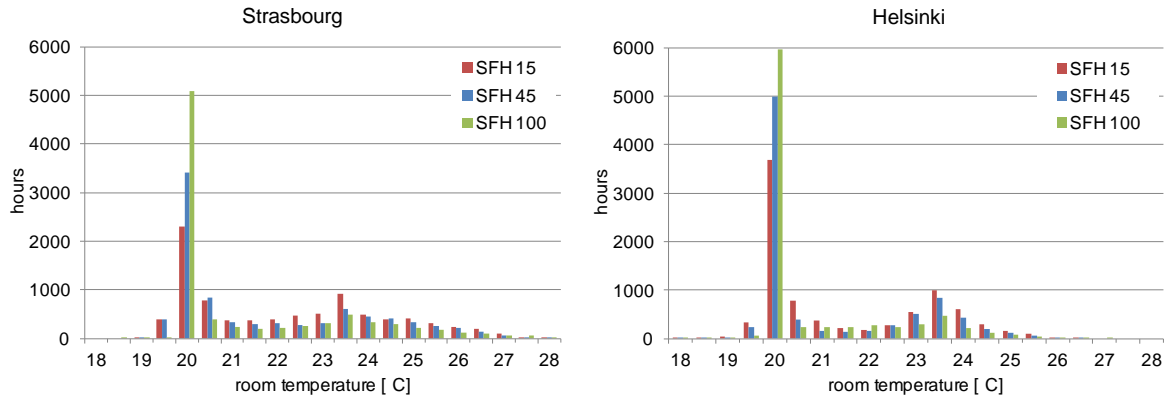


Figure 9: Yearly occurrence of room temperatures (hourly averages) for the different buildings in the climates of Strasbourg and Helsinki.

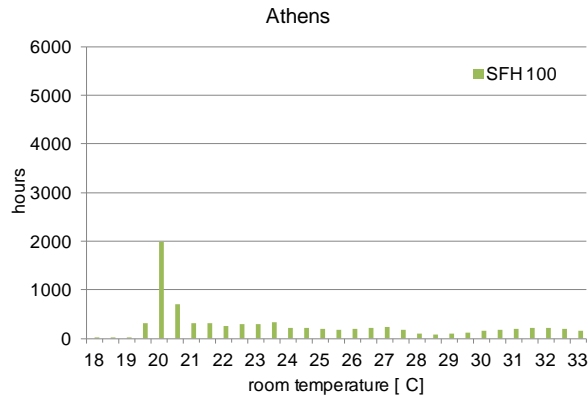


Figure 10: Yearly occurrence of room temperatures (hourly averages) for the SFH 100 building in the climate of Athens.

The room temperature plots have been obtained for the 0.5 K – discretized x-axis values by counting the number of hours where the average room temperature was ± 0.25 of these x-axis values.

6.3 Monthly Heat loads

The heat load calculation is based on the input and output temperatures and mass flows of the space heating system (floor heating or radiator). The space heat loads for the different buildings in the climates of Strasbourg and Helsinki are shown in Figure 11, and the heat load for the SFH100 building in the climate of Athens is shown in Figure 12.

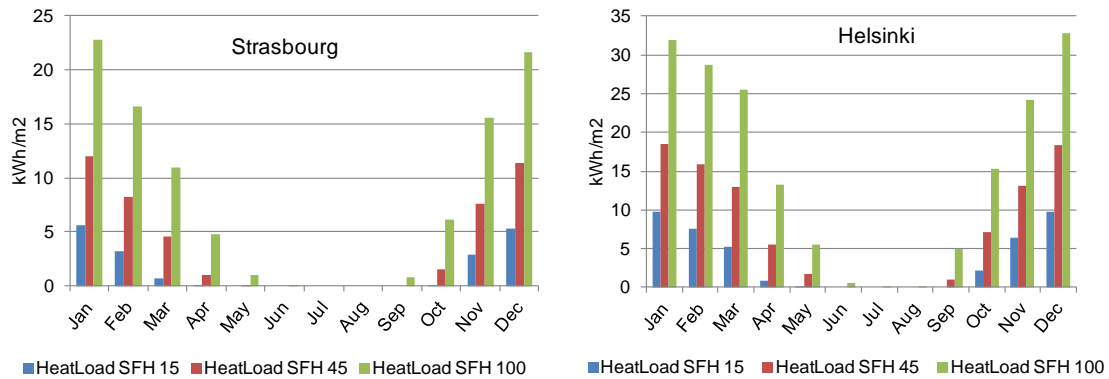


Figure 11: Monthly heat loads of the space heat distribution system for the different buildings in the climates of Strasbourg and Helsinki.

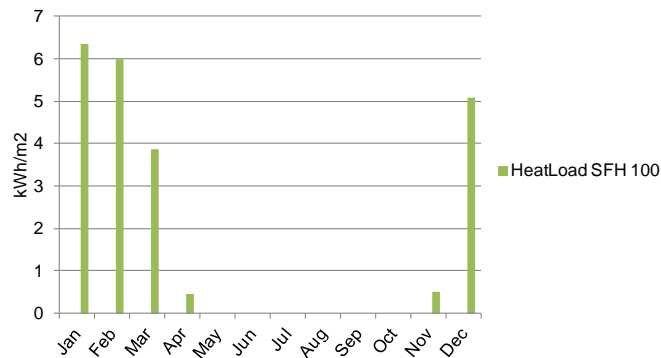


Figure 12: Monthly heat loads of the space heat distribution system for the SFH 100 building in the climate of Athens.

6.4 Flow and return temperatures

The flow and return temperatures of the heating system for the different buildings in the different climates are shown in Figure 13. The red (b/w: dark) curves show how much heat is delivered with *flow temperatures* below a certain temperature level. The blue (b/w: light) curves show how much heat is delivered with *return temperatures* below a certain temperature level. From the diagram of the SFH 100 in the climate of Strasbourg it can be seen that the space heating load is 14 MWh/a, and that about 6 MWh are delivered with flow temperatures below 40 °C.

For the comparison of solar and heat pump system performance, these are the most important curves that two different simulations have to match in order to be comparable!

Seasonal performance factors can be improved considerably by assuming lower flow and return systems of the space heating system only, without improving the system that delivers the heat.

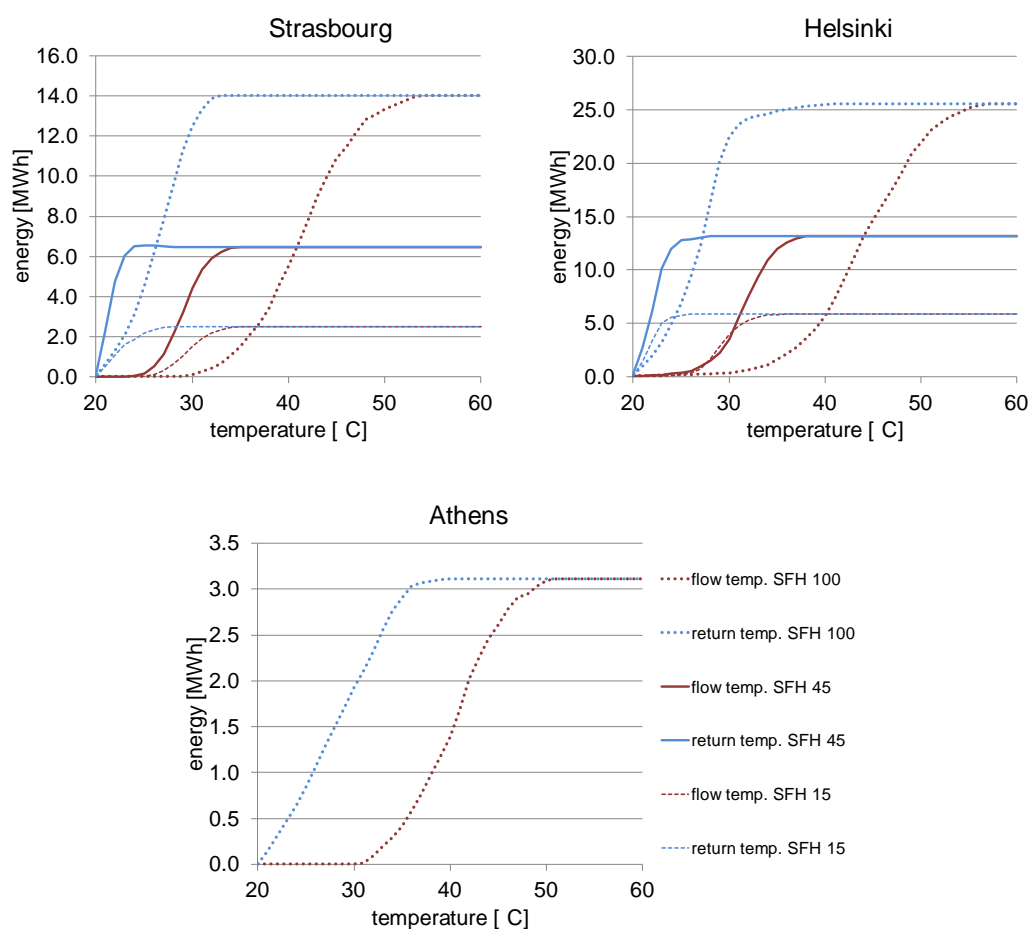


Figure 13: Monthly heat loads of the space heat distribution system for the different buildings in the climates of Strasbourg, Helsinki and Athens.

The presented temperature-curves for the flow and return of the heating system are based on hourly averaged values of the heating power $\dot{Q}_{Rd} = \dot{m} \cdot c_p \cdot (\vartheta_{Rd,in} - \vartheta_{Rd,out})$ and the hourly averaged values of the inlet and outlet temperatures (i.e. of $\vartheta_{Rd,in}$ and $\vartheta_{Rd,out}$) of the radiator or floor heating system. For each temperature ϑ_x on x-axis of the plot the y-axis value is obtained by integrating \dot{Q}_{Rd} of all hours of the year where $\vartheta_{Rd,in} \leq \vartheta_x$.

6.5 Tabular values of monthly building simulation results

The transmission losses shown do not include ground heat exchange losses since these are shown separately.

6.5.1 Strasbourg

Table 11: Simulation results for the SFH 15 in the climate of Strasbourg.

	Heat Load	Solar Gains	Transm. Loss	Air Flow Loss	Ground Heat Exch.	T_{room}	$T_{FI,Avg}$	$T_{Rt,Avg}$
	kWh/m ²	°C	°C	°C				
Jan	5.626	2.080	6.769	2.050	-0.935	20.1	30.5	24.0
Feb	3.169	3.082	5.415	1.695	-0.878	20.1	29.3	21.7
Mar	0.665	4.698	4.868	1.591	-0.908	20.6	27.7	20.6
Apr	0.002	4.679	4.043	1.602	-0.732	22.0	27.7	20.7
May	0.000	3.589	2.745	2.168	-0.556	23.5	0.0	0.0
Jun	0.000	2.738	1.622	2.587	-0.351	24.6	0.0	0.0
Jul	0.000	2.569	1.362	2.944	-0.227	24.9	0.0	0.0
Aug	0.000	2.328	1.349	2.691	-0.186	25.1	0.0	0.0
Sep	0.000	2.660	2.034	2.575	-0.245	23.5	0.0	0.0
Oct	0.034	3.608	3.578	1.754	-0.408	21.7	27.7	20.6
Nov	2.838	2.354	4.790	1.595	-0.588	20.1	28.4	21.2
Dec	5.333	1.790	6.366	1.941	-0.801	20.1	29.8	23.5
Total	17.669	36.175	44.942	25.192	-6.816	22.2		

Table 12: Simulation results for the SFH 45 in the climate of Strasbourg.

	Heat Load	Solar Gains	Transm. Loss	Air Flow Loss	Ground Heat Exch.	T_{room}	$T_{FI,Avg}$	$T_{Rt,Avg}$
	kWh/m ²	°C	°C	°C				
Jan	11.994	2.355	10.125	5.111	-1.169	20.0	30.1	22.2
Feb	8.177	3.495	8.204	4.219	-1.099	20.0	29.1	21.4
Mar	4.531	5.347	7.048	3.628	-1.138	20.1	27.4	20.7
Apr	0.964	5.845	5.055	2.722	-0.916	20.6	26.1	20.4
May	0.025	5.072	3.944	2.144	-0.695	22.5	27.2	20.5
Jun	0.000	3.485	2.443	2.430	-0.436	24.4	0.0	0.0
Jul	0.000	2.953	2.005	2.641	-0.279	24.6	0.0	0.0
Aug	0.000	2.683	1.912	2.429	-0.227	24.8	0.0	0.0
Sep	0.000	3.834	3.180	2.579	-0.300	23.0	0.0	0.0
Oct	1.549	4.353	4.831	2.658	-0.504	20.5	26.4	20.5
Nov	7.616	2.665	7.418	3.971	-0.732	20.0	28.1	21.0
Dec	11.399	2.025	9.515	4.838	-0.999	20.0	29.4	22.0
Total	46.255	44.114	65.680	39.370	-8.496	21.7		

Table 13: Simulation results for the SFH 100 in the climate of Strasbourg.

	Heat Load	Solar Gains	Transm. Loss	Air Flow Loss	Ground Heat Exch.	T_{room}	$T_{FI,Avg}$	$T_{Rt,Avg}$
	kWh/m ²	°C	°C	°C				
Jan	22.805	2.739	21.409	5.106	-1.042	20.0	44.7	34.1
Feb	16.615	4.065	17.310	4.210	-1.021	20.0	42.7	31.0
Mar	10.949	6.213	14.527	3.606	-1.110	20.1	38.8	27.4
Apr	4.820	6.771	9.986	2.648	-0.952	20.3	35.7	24.4
May	0.955	6.300	6.628	1.837	-0.782	21.7	33.4	22.6
Jun	0.007	4.847	4.169	2.114	-0.542	24.0	29.3	20.6
Jul	0.000	3.995	3.678	1.970	-0.378	24.3	0.0	0.0
Aug	0.000	3.701	3.409	2.026	-0.284	24.6	0.0	0.0
Sep	0.842	5.045	5.596	1.970	-0.296	21.7	31.5	21.8
Oct	6.085	5.062	10.178	2.575	-0.436	20.2	35.2	25.5
Nov	15.536	3.100	16.001	3.963	-0.618	20.0	40.3	29.9
Dec	21.604	2.355	20.260	4.832	-0.860	20.0	43.3	33.4
Total	100.218	54.193	133.151	36.857	-8.320	21.4		

6.5.2 Helsinki

Table 14: Simulation results for the SFH 15 in the climate of Helsinki.

	Heat Load	Solar Gains	Transm. Loss	Air Flow Loss	Ground Heat Exch.	T_{room}	$T_{FI,Avg}$	$T_{Rt,Avg}$
	kWh/m ²	°C	°C	°C				
Jan	9.745	1.167	9.049	2.713	-1.230	19.8	30.0	22.6
Feb	7.511	2.858	8.459	2.566	-1.180	19.9	30.5	22.2
Mar	5.198	4.737	8.153	2.506	-1.265	20.1	29.5	21.0
Apr	0.815	5.628	5.477	1.793	-1.075	20.4	27.2	20.3
May	0.074	5.783	4.787	1.871	-0.885	22.2	26.7	20.1
Jun	0.000	3.798	2.570	2.519	-0.627	23.6	0.0	0.0
Jul	0.000	3.145	1.922	2.651	-0.464	24.2	0.0	0.0
Aug	0.000	2.819	2.026	2.542	-0.381	23.8	0.0	0.0
Sep	0.000	3.573	3.445	1.834	-0.412	22.5	0.0	0.0
Oct	2.231	3.101	5.064	1.702	-0.582	20.3	27.1	20.7
Nov	6.440	1.221	6.648	2.049	-0.784	20.0	28.0	21.3
Dec	9.740	0.710	8.672	2.602	-1.046	20.0	29.4	22.3
Total	41.755	38.540	66.272	27.348	-9.931	21.4		

Table 15: Simulation results for the SFH 45 in the climate of Helsinki.

	Heat Load	Solar Gains	Transm. Loss	Air Flow Loss	Ground Heat Exch.	T_{room}	$T_{FI,Avg}$	$T_{Rt,Avg}$
	kWh/m ²	°C	°C	°C				
Jan	18.569	1.319	13.536	6.689	-1.723	19.5	31.8	23.1
Feb	15.834	3.227	12.878	6.369	-1.642	19.7	32.6	23.0
Mar	13.019	5.381	12.491	6.253	-1.741	20.0	32.2	21.9
Apr	5.591	6.415	8.228	4.277	-1.458	20.1	29.1	20.8
May	1.724	7.475	6.560	3.147	-1.173	21.1	27.8	20.5
Jun	0.000	5.384	3.839	2.665	-0.806	23.3	0.0	0.0
Jul	0.000	3.906	2.838	2.362	-0.577	24.0	0.0	0.0
Aug	0.000	3.802	3.163	2.294	-0.473	23.5	0.0	0.0
Sep	0.961	4.937	4.741	2.791	-0.536	21.3	26.9	20.3
Oct	7.139	3.510	7.742	4.008	-0.794	20.1	28.8	21.0
Nov	13.056	1.379	10.054	5.123	-1.092	20.0	30.6	21.8
Dec	18.372	0.800	13.118	6.489	-1.468	19.9	32.2	22.9
Total	94.265	47.535	99.188	52.465	-13.483	21.0		

Table 16: Simulation results for the SFH 100 in the climate of Helsinki.

	Heat Load	Solar Gains	Transm. Loss	Air Flow Loss	Ground Heat Exch.	T_{room}	$T_{FI,Avg}$	$T_{Rt,Avg}$
	kWh/m ²	°C	°C	°C				
Jan	31.906	1.533	27.389	6.405	-1.508	18.5	44.2	28.9
Feb	28.686	3.755	26.515	6.250	-1.488	19.2	47.3	28.3
Mar	25.444	6.255	25.910	6.254	-1.656	20.0	46.0	26.2
Apr	13.259	7.449	16.999	4.263	-1.480	20.0	39.9	23.7
May	5.493	9.217	12.427	3.021	-1.297	20.7	36.8	22.6
Jun	0.581	7.252	6.659	2.161	-0.989	22.1	31.9	20.7
Jul	0.006	5.492	4.933	1.819	-0.779	23.4	28.3	20.4
Aug	0.029	6.150	5.787	1.804	-0.631	22.5	29.3	20.5
Sep	5.004	5.992	9.816	2.550	-0.603	20.6	34.5	22.2
Oct	15.231	4.083	16.614	3.997	-0.754	20.0	38.9	24.4
Nov	24.154	1.604	21.607	5.122	-0.957	20.0	42.7	26.6
Dec	32.817	0.931	27.968	6.483	-1.264	19.9	46.0	28.8
Total	182.610	59.713	202.626	50.128	-13.404	20.6		

6.5.3 Athens

Table 17: Simulation results for the SFH 100 in the climate of Athens.

	Heat Load	Solar Gains	Transm. Loss	Air Flow Loss	Ground Heat Exch.	T_{room}	$T_{FI,Avg}$	$T_{Rt,Avg}$
	kWh/m ²	°C	°C	°C				
Jan	6.350	6.984	12.123	2.878	-0.402	20.2	41.3	29.1
Feb	5.986	5.885	10.685	2.577	-0.483	20.2	41.6	29.6
Mar	3.865	6.331	9.299	2.375	-0.564	20.4	38.9	26.3
Apr	0.451	6.158	6.323	1.761	-0.466	21.4	34.6	22.0
May	0.000	3.632	3.467	1.904	-0.305	24.7	0.0	0.0
Jun	0.000	3.177	2.805	2.209	-0.080	29.1	0.0	0.0
Jul	0.000	3.165	3.049	2.201	0.126	32.1	0.0	0.0
Aug	0.000	2.911	2.872	2.294	0.266	32.0	0.0	0.0
Sep	0.000	2.678	2.528	2.404	0.287	27.7	0.0	0.0
Oct	0.000	3.497	3.944	1.780	0.210	24.0	0.0	0.0
Nov	0.517	5.937	6.736	1.695	0.030	21.4	36.2	23.3
Dec	5.077	5.531	10.041	2.386	-0.192	20.2	39.7	28.8
Total	22.247	55.886	73.872	26.464	-1.571	24.5		

7 Symbols

Symbols

c_p	specific heat, J/kgK
g	gravitation of the earth, 9.81 m/s ²
H	height, m
\dot{m}	mass flow rate, kg/s
n_{Rd}	radiator exponent, -
\dot{Q}	(heating) power, W
R	overall resistance, m ² K/W
T	temperature, K
U	overall heat transfer coefficient, W/m ² K
\dot{V}	volume flow rate, m ³ /h
W	width, m
α_c	surface heat transfer coefficient, W/m ² K
α	angle, °
$\Delta\theta_i$	amplitude of the sine curve that describes the temperature difference between the inside and the outside, K
$\bar{\theta}_i$	annual average inside air temperature, °C
ϑ	temperature, °C
λ_{eff}	heat exchanger effectiveness, -
v_{wind}	wind speed from climate data, m/s

Subscript

<i>air</i>	„free stream“ air
<i>amb</i>	ambient outside air
<i>AT</i>	Athens
<i>Avg</i>	average
<i>d</i>	at design conditions
<i>DA</i>	Davos
<i>Fl</i>	flow line
<i>HE</i>	Helsinki
<i>HS</i>	heating season
<i>in</i>	inlet of a device
<i>loc</i>	for the local climate
<i>MT</i>	Montreal
<i>out</i>	outlet of a device
<i>Rd</i>	radiator / floor heating system
<i>Rt</i>	return line
<i>room</i>	air of the room inside the building
<i>ST</i>	Strasbourg
<i>surface</i>	surface

8 References

- Directive 2009/125/EC of the European Parliament and of the Council of 21 October 2009 establishing a framework for the setting of ecodesign requirements for energy-related products (recast).
- EN ISO 6946:2007 - Building components and building elements - Thermal resistance and thermal transmittance - Calculation method, International Organization for Standardization ISO, Geneva.
- Feist, W., 2005. First Steps: What can be a Passive House in your region with your climate?, Passive House Institute (www.passiv.de), Darmstadt.
- Glück B., 2007. Wärmeübergangskoeffizienten an thermisch aktiven Bauteiloberflächen und der Übergang zu Basiskennlinien für die Wärmestromdichte; gi Gesundheits-Ingenieur; 128. Jahrgang 2007, Heft 1, Seiten 1-10
- Haller, M., Dott, R., Ruschenburg, J., Ochs, F. & Bony, J., 2012. The Reference Framework for System Simulations of the IEA SHC Task 44 / HPP Annex 38 - Part A: General Boundary Conditions - A technical Report of Subtask C. Report C1, Institut für Solartechnik SPF, Hochschule für Technik HSR, Rapperswil, Switzerland.
- Heimrath, R. & Haller, M., 2007. The Reference Heating System, the Template Solar System of Task 32, IEA Solar Heating and Cooling program – Task 32, Graz.
- Martin, M., Berdahl, P., 1984. Characteristics of Infrared Sky radiation in the United States, Lawrence Berkley Laboratory, University of California - berkley, Solar energy Vol. 33, No.3 / 4, pp.321-336.
- Minergie, 2010. The MINERGIE®-Standard for Buildings - Planning and project: Informations for architects, Association Minergie (www.minergie.ch), Bern.
- Perez, R., Ineichen, P., Seals, R., Michalsky, J., Stewart, R., 1990. Modeling daylight availability and irradiance components from direct and global irradiance. Solar Energy 44, 271-289.

Appendix A: Temperature distribution and ambient design temperature

Since no published design outdoor temperatures on an identical basis have been found for the chosen locations, the outdoor design temperature is defined as the lowest temperature to lie in the $z=2.57\sigma$ quantile (i.e. the confidence interval of $p=0.99$ ($p(z) = \text{erf}(2^{-1/2} z)$)) with respect to the lowest temperature of the yearly temperature variation (sine fit) of the location.

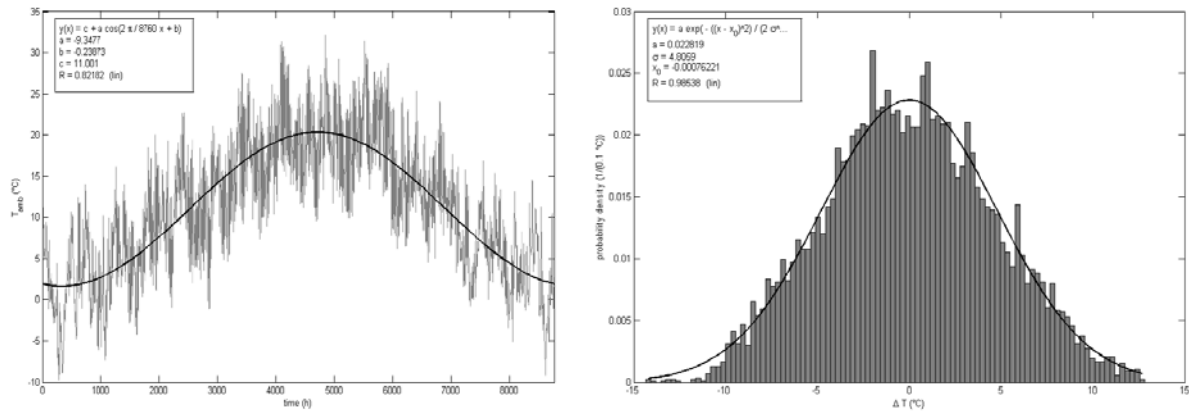


Figure 14: Left: temperature distribution for Strasbourg, with sine fit (black curve); right: probability density distribution of temperature deviation from sine fit for Strasbourg, with gauss fit (black curve).

Appendix B: Long-wave radiation heat exchange with the sky

The long-wave heat transfer emission is calculated with the Stefan-Boltzmann law where for the temperature the sky temperature T_{sky} calculated using the correlation from Martin & Berdahl (1984):

$$T_{sky} = T_{amb} \left(\varepsilon_0 + e^{-\frac{h_c}{8200m}} \cdot (1 - \varepsilon_0) \cdot C_{cover} \right)^{0.25} \quad (1)$$

where C_{cover} is the cloudiness factor of the sky, h_c the cloud height (in TRNSYS assumed with 1830 m) and ε_0 the emittance of the clear sky which is derived from the saturation temperature ϑ_{sat} by:

$$\varepsilon_0 = 0.711 + 0.0056 \cdot \vartheta_{sat} + 7.3 \cdot 10^{-5} \cdot \vartheta_{sat}^2 + 12 \cdot 10^{-5} (p_{atm} - p_0) \quad (2)$$

where p_{atm} is the station pressure in millibar and p_0 the reference station pressure of 1000 millibar.

Appendix C: Heat load estimation

The heat load at design ambient temperature is calculated as an extrapolation of a linear fit to the daily heating power consumption.

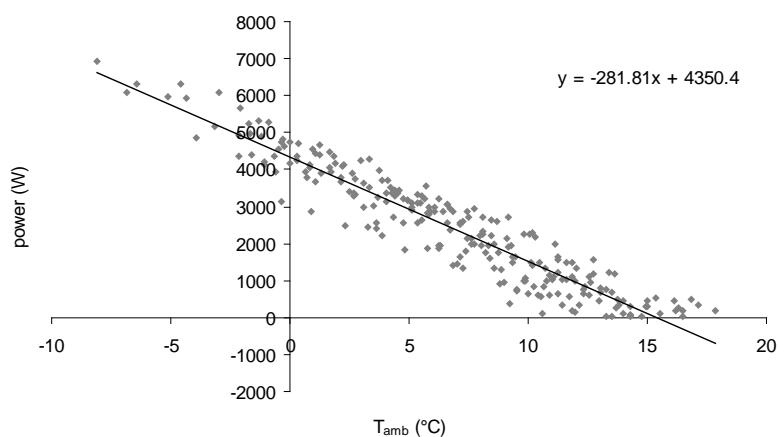


Figure 15: Daily heating power consumption as a function of ambient temperature for SFH100 at Strasbourg, with linear fit (black curve).

Appendix D: Ground Coupling Heat Losses (TRNSYS Type 985)

Introduction

This TRNSYS Type calculates the undisturbed ground temperature based on ground and climate values as well as simplified ground coupling heat losses of buildings according to (ISO/DIS 13370 2005) – slab on ground.

Parameters

Nr.	short	explanation	unit	range
1	$\bar{\theta}_e$	average outside temperature over the year (solar or snow influence on ground surface temperature may be included here)	°C	[inf;+inf]
2	$\Delta\theta_e$	amplitude of sine-curve that approximates the outside temperature variation over one year	K	[0;+inf]
3	t_{shift}	time-shift of lowest temperature in the year based on the sine-curve that approximates the outside temperature over the year	h	[0;+inf]
4	λ_{grd}	conductivity of the ground	W/mK	[0;+inf]
5	ρ_{grd}	density of the ground	kg/m ³	[0;+inf]
6	cP_{grd}	heat capacity of the ground	kJ/kgK	[0;+inf]
7	G_t	geothermal gradient	K/m	[0;+inf]
8	z_{grd1}	depth 1 for the evaluation of the undisturbed ground temperature	m	[0;+inf]
9	z_{grd2}	depth 2 for the evaluation of the undisturbed ground temperature	m	[0;+inf]
10	z_{grd3}	depth 3 for the evaluation of the undisturbed ground temperature	m	[0;+inf]
11	$\bar{\theta}_i$	average inside temperature over the year	°C	[-inf;+inf]
12	$\Delta\theta_i$	amplitude of sine-curve that approximates the inside temperature variation over one year	K	[0;+inf]
13	l_{floor}	length of the floor in contact with the ground	m	[0;+inf]
14	b_{floor}	width of the floor in contact with the ground	m	[0;+inf]
15	w	thickness of the walls around the floor in contact with the ground	m	[0;+inf]
16	R_{tot}	total thermal resistance of floor with inside and outside coefficients ($= R_{si} + R_f + R_{se}$)	Km ² /W	[0;+inf]
17	ψ_g	Linear thermal transmittance associated with wall/floor junction	W/mK	[0;+inf]

Inputs

Nr.	short	explanation	unit	range
-----	-------	-------------	------	-------

No inputs. The only time-dependent variable is the time of the year itself – and this will be taken directly from TRNSYS.

Outputs

Nr.	short	explanation	unit	range
1	t_{z1}	undisturbed soil temperature at depth 1	°C	[-inf;+inf]
2	t_{z2}	undisturbed soil temperature at depth 2	°C	[-inf;+inf]
3	t_{z3}	undisturbed soil temperature at depth 3	°C	[-inf;+inf]
4	\dot{Q}_{ground}	ground coupling heat exchange, positive values are heat gains from the ground, negative values are heat losses to the ground	kJ/h	[-inf;+inf]
5	δ_{grd}	periodic penetration depth	m	[0;+inf]
6	d_t	equivalent thickness of ground representing thermal resistance of the floor	m	[0;+inf]
7	α	additional time-shift for inside temperature variation	h	[0;+inf]
8	β	additional time-shift for external temperature variation	h	[0;+inf]

Calculation

General equation for undisturbed ground temperature

The temperature of the undisturbed ground ($\mathcal{G}_{grd,\infty}$) is simulated as a function of the time of the year (t) and the depth (z) according to Eq. 1 that is based on approaches presented in the literature for seasonal temperature variations in the earth's crust (Baehr & Stephan 2006; Wesselak & Schabbach 2009), neglecting the influence of the heat transfer resistance from the ambient air to the surface of the ground (i.e. $\alpha_{surf} = \infty$):

$$\text{Eq. 1} \quad \mathcal{G}_{grd,\infty}(t, z) = \bar{\theta}_e - \Delta\theta_e \cdot \text{EXP}\left(-\frac{z}{\delta_{grd}}\right) \cdot \text{COS}\left[2 \cdot \pi \cdot \frac{(t - t_{shift})}{t_0} - \frac{z}{\delta_{grd}}\right] + G_t \cdot z_{grd}$$

General equation for ground coupling heat losses

Simplified ground coupling losses are calculated with Eq. 2 that is based on an approach presented in (ISO/DIS 13370 2005). Positive values of \dot{Q}_{ground} correspond to heat gains from the ground, negative values to heat losses to the ground.

$$\text{Eq. 2} \quad \dot{Q}_{ground} = L_s \cdot (\bar{\theta}_e - \bar{\theta}_i) - L_{pi} \cdot \Delta\theta_i \cdot \cos\left(2\pi \frac{t - t_{shift} - \alpha}{t_0}\right) - L_{pe} \cdot \Delta\theta_e \cdot \cos\left(2\pi \frac{t - t_{shift} - \beta}{t_0}\right)$$

Thermal penetration depth of the ground

$$\text{Eq. 3} \quad \delta_{grd} = \sqrt{\frac{t_0 \cdot 3600 \text{ s/h} \cdot \lambda_{grd}}{\pi \cdot \rho_{grd} \cdot c p_{grd}}}$$

Slab on ground heat loss calculations

$$\text{Eq. 4} \quad A_{floor} = l_{floor} \cdot b_{floor}$$

$$\text{Eq. 5} \quad P_{floor} = 2 \cdot l_{floor} + 2 \cdot b_{floor}$$

$$\text{Eq. 6} \quad B_{floor} = 2 \cdot A_{floor} / P_{floor}$$

$$\text{Eq. 7} \quad d_t = w + \lambda_{grd} \cdot R_{tot}$$

$$\text{Eq. 8} \quad \alpha = \left[1.5m - \frac{12m}{2 \cdot \pi} \cdot \arctan\left(\frac{d_t}{d_t + \delta_{grd}}\right) \right] \cdot \frac{8760h}{12m}$$

$$\text{Eq. 9} \quad \beta = \left[1.5m - 0.42m \cdot \ln\left(\frac{\delta_{grd}}{d_t} + 1\right) \right] \cdot \frac{8760h}{12m}$$

$$\text{Eq. 10} \quad R_{grd} = 0.457 \cdot B_{floor} / \lambda_{grd}$$

$$\text{Eq. 11} \quad U_{steady} = 1 / (R_{tot} + w / \lambda_{grd} + R_{grd})$$

$$\text{Eq. 12} \quad L_s = A_{floor} \cdot U_{steady} + \psi_g \cdot P_{floor}$$

$$\text{Eq. 13} \quad L_{pi} = A_{floor} \cdot \frac{\lambda_{grd}}{d_t} \cdot \sqrt{\frac{2}{(1 + \delta_{grd} / d_t)^2 + 1}}$$

$$\text{Eq. 14} \quad L_{pe} = 0.37 \cdot P_{\text{floor}} \cdot \lambda_{\text{grd}} \cdot LN \left(\frac{\delta_{\text{grd}}}{d_t} + 1 \right)$$

Floor heating system

In the case of floor heating instead of the internal temperature, the temperature of the floor heating system should be taken:

$$\text{Eq. 15} \quad \theta_i = 0.5 \cdot (\theta_{\text{floor},in} + \theta_{\text{floor},out})$$

A simplified procedure for an approximate calculation of $\bar{\theta}_i$ and $\Delta\theta_i$ in the case of a floor heating system is presented here with Eq. 16 - Eq. 18.

$$\text{Eq. 16} \quad \theta_{i,max} = 20 + \left(\frac{(\theta_{fl,nom} + \theta_{rt,nom})}{2} - 20 \right) \cdot \frac{20 - (\bar{\theta}_e - \Delta\theta_e)}{20 - \theta_{amb,d}}$$

$$\text{Eq. 17} \quad \bar{\theta}_i = (20 + \theta_{i,max}) / 2$$

$$\text{Eq. 18} \quad \Delta\theta_i = \theta_{i,max} - \bar{\theta}_i$$

Symbols

B_{floor}	characteristic dimension of floor, m
d_t	total equivalent thickness of the floor (thickness of ground that has the same thermal resistance as the floor), m
L_s	steady state thermal coupling coefficient, W/K
L_{pi}	internal periodic thermal coupling coefficient, W/K
L_{pe}	external periodic thermal coupling coefficient, W/K
P_{floor}	perimeter of the floor, m
Q_{ground}	ground heat flow, W
R_f	heat transfer resistance of floor, m ² K/W
R_{si}, R_{se}	inners surface resistance, external surface resistance, m ² K/W
R_{grd}	effective thermal resistance of the ground, m ² K/W
t	time of the year, h
t_0	total hours of one year (= 8760 h)
t_{shift}	hour of the year in which the external temperature sine-curve fit shows a minimum, h
w	thickness of (side) walls, including all layers, m
α, β	phase shifts, h
$\bar{\theta}_i, \bar{\theta}_e$	annual average internal (i) and external / ambient temperature (e), °C
$\Delta\theta_i, \Delta\theta_e$	amplitude of variations of monthly mean internal / ambient temperatures, °C
$\theta_{i,max}$	maximum temperature of sine-fit for temperature of heated floor in contact with ground, °C

- $\theta_{fl,nom}$, $\theta_{rt,nom}$ nominal flow and return temperature of the floor heating system at ambient temperature
- $\theta_{amb,d}$ ambient design temperature for the heating system, °C
- δ_{grd} periodic penetration depth (depth at which the amplitude of the temperature sine-curve is $1/e \approx 37\%$ of its surface value), m

Acknowledgements

Thanks goes to Fabian Ochs / Universität Innsbruck – for providing information on the calculation based on ISO 13370 and undisturbed soil temperature calculation in general.

References of Appendix D

Baehr, H.D. & Stephan, K., 2006. Heat and mass transfer, Second Edition. Springer, Berlin.

ISO/DIS 13370, 2005. Thermal performance of buildings — Heat transfer via the ground — Calculation methods.

Wesselak, V. & Schabbach, T., 2009. Regenerative Energietechnik, 1st ed. Springer, Berlin.

Appendix E: Return temperature control of heat distribution / heat pump

$$g_{out} = g_{set} - \frac{g_{d,in} - g_{d,out}}{2} \cdot \frac{g_{set} - g_{amb24}}{g_{set} - g_{ambD}} + \left(\frac{g_{d,in} + g_{d,out}}{2} - g_{set} \right) \cdot \left(\frac{g_{set} - g_{amb24}}{g_{set} - g_{ambD}} \right)^{\frac{1}{n_{Rd}}}$$

Where:

g_{out} = Temp. of return (calculated), °C

g_{set} = setpoint indoor temperature, °C

$g_{d,in}$ = Temp. of flow at design ("normal") conditions, °C

$g_{d,out}$ = Temp. of return at design conditions, °C

g_{amb24} = 24 hour averaged outdoor temperature, °C

g_{ambD} = Design outdoor temperature, °C

n_{Rd} = Radiator exponent, -

Appendix F: Changelog since first version of April 2012

- The radiative heat fraction of the heat emitting system was changed from 0.35 to 0.0 (section 5.1.1).
- A standard pressure drop of 0.3 bar for the space heat distribution loop was introduced (section 5)
- The reference mass flow rate control for all systems has been set to thermostatic valves (mass flow variable between 0-100% of the nominal mass flow according to room temperatures).
- The calculation of the supply temperature setpoint has been updated with version 2 that was also used for the reference simulations.
- The wording of the description of the heat emission systems has been adapted in order to make things clearer.
- Calculation of return temperature setpoint has been added.
- Correction of equations numbering and referencing, correction of typos.
- References to Appendix A and C have been added in the text.
- the electric gains profile was erroneously referred to as a weekly profile on page 11 -> changed to "daily" profile.